

Deuteron Spin Structure Functions at Small Bjorken- x [†]

J. Edelmann, G. Piller and W. Weise

Physik Department, Technische Universität München,
D-85747 Garching, Germany

Abstract

We investigate polarized deuteron structure functions at small values of the Bjorken variable, $x < 0.1$. In this region contributions from the coherent interaction of diffractively excited hadronic states with both nucleons become important. A proper treatment of this process requires an extension of the Glauber-Gribov multiple scattering theory to include spin degrees of freedom. In the kinematic domain of current fixed target experiments we observe that shadowing effects in g_1^d are approximately twice as large as for the unpolarized structure function F_2^d . Furthermore at $x < 0.1$ the tensor structure function b_1 is found to receive significant contributions from coherent double scattering.

PACS: 13.60.Hb, 24.70.+s, 25.30.Mr

[†]Work supported in part by BMBF

I. INTRODUCTION

In recent years polarized deep-inelastic scattering experiments have become a major topic at all high energy lepton beam facilities. They aim primarily at the investigation of the spin structure of hadrons. Here the use of proton targets has led to detailed information about the spin structure function g_1^p . In addition the corresponding neutron structure function g_1^n has been explored. Combined with proton data the latter is crucial for the extraction of the flavor singlet combination of polarized quark distributions, and for testing the fundamental Bjorken sum rule.

To investigate neutron structure functions nuclear targets are needed. In current experiments at CERN [1], SLAC [2,3] and HERMES [4], ^3He and deuteron targets are used. For an accurate extraction of neutron structure functions a detailed knowledge of nuclear effects is therefore required. At moderate and large values of the Bjorken variable, $x > 0.2$, such effects can be traced back to nuclear binding and Fermi motion (see e.g. [5] and references therein). At small $x < 0.1$ corrections due to coherent multiple scattering processes become important. In unpolarized deep-inelastic scattering these are responsible for nuclear shadowing which has been established in recent experiments at FNAL [6,7] and CERN [8] as a leading twist effect.

In this paper we study polarized deep-inelastic scattering from deuterium at small x . Important contributions to the corresponding cross section come from mechanisms in which the exchanged virtual photon scatters diffractively from one of the nucleons in the target and produces hadronic intermediate states which subsequently interact with the second nucleon. Coherent double scattering is described by the Glauber-Gribov multiple scattering theory which we extend in the present work to include spin degrees of freedom.

We estimate shadowing effects in the deuteron spin structure function g_1^d . The corrections thus obtained turn out to be approximately a factor two larger than those for the unpolarized structure function F_2^d . Nevertheless, as compared to other uncertainties in the extraction of g_1^n from deuteron data, these corrections are relatively small.

Because of its spin-1 nature the deuteron is characterized by additional structure functions as compared to a free nucleon. Amongst those the yet unmeasured structure function b_1 [9–11] will be investigated at HERMES [12]. Model calculations suggest that b_1 is very small at moderate and large $x > 0.2$ (see e.g. [13]). At small $x < 0.1$ dominant contributions to b_1 result from coherent double scattering processes. Here the magnitude of b_1 reaches around 2% of the unpolarized nucleon structure function F_1^N . This interesting effect is entirely due to an interference between the S - and D -state component in the deuteron wave function.

First investigations of double scattering contributions to polarized deuteron structure functions have been performed in [14] within a Regge model. However, in that work an unrealistic deuteron wave function has been used neglecting the D -state component. At $x < 0.1$ the latter turns out to be crucial for a proper estimate of the structure function b_1 as found in [15,16] (see also [17,18]). Shadowing effects for spin structure functions have been discussed recently within the framework of a simple model, especially for ^3He targets [19]. The magnitude of the observed effect agrees well with the results presented here.

This paper is organized as follows: in Sec.II we recall the relationship between structure functions and photon helicity amplitudes. An extension of the Glauber-Gribov multiple

scattering series to spin degrees of freedom is presented in Sec.III, where we also derive the single and double scattering contributions to deuteron structure functions. In Sec.IV we estimate shadowing effects in the spin structure function g_1^d and discuss implications for the extraction of the neutron structure function g_1^n . Results for b_1 are presented in Sec.V. We summarize in Sec.VI.

II. STRUCTURE FUNCTIONS AND HELICITY AMPLITUDES

In inclusive deep-inelastic lepton scattering one probes the hadronic tensor

$$W_{\mu\nu}(p, q, s) = \frac{1}{4\pi} \int d^4\xi e^{iq\cdot\xi} \langle p, s | J_\mu(\xi) J_\nu(0) | p, s \rangle \quad (1)$$

of the target. Here J^μ is the electromagnetic current. The four-momenta of the target and the exchanged photon are labeled by p^μ and $q^\mu = (q_0, \mathbf{q})$, respectively. The spin vector s^μ is orthogonal to the target momentum, $p \cdot s = 0$, and normalized such that $s^2 = -M_T^2$, where M_T is the invariant mass of the target. For a spin-1/2 target s^μ directly represents the target polarization, while for a spin-1 target it is defined in terms of the polarization vectors \mathcal{E}_H as $s_\alpha(H) = -i\varepsilon_{\alpha\beta\gamma\delta} \mathcal{E}_H^{\beta*} \mathcal{E}_H^\gamma p^\delta$, where $H = 0, +1, -1$ (abbreviated as $0, +, -$) denotes the spin projection along the quantization axis.

According to the optical theorem inclusive deep-inelastic lepton scattering can be described in terms of the forward scattering of a virtual photon. The corresponding Compton amplitude is given by:

$$T_{\mu\nu}(p, q, s) = i \int d^4\xi e^{iq\cdot\xi} \langle p, s | T(J_\mu(\xi) J_\nu(0)) | p, s \rangle. \quad (2)$$

A comparison with Eq.(1) gives:

$$W_{\mu\nu} = \frac{1}{2\pi} \text{Im} T_{\mu\nu}. \quad (3)$$

Using the Compton tensor one can define photon-target forward helicity amplitudes (Fig.1):

$$\mathcal{A}_{jH,j'H'} = e^2 \varepsilon_{j'}^{*\mu} T_{\mu\nu}(H', H) \varepsilon_j^\nu, \quad (4)$$

with the electromagnetic coupling $e^2/4\pi = 1/137$. The helicities of the incoming and scattered photon are labeled by j and j' . Choosing the photon momentum in the longitudinal direction, $q^\mu = (q_0, \mathbf{0}_\perp, q_z)$ with $q_z > 0$, gives for the photon polarization vectors $\varepsilon_+^\mu = (0, -1, -i, 0)/\sqrt{2}$, $\varepsilon_-^\mu = (0, 1, -i, 0)/\sqrt{2}$ and $\varepsilon_0^\mu = (q_z, 0, 0, q_0)/\sqrt{-q^2}$. Furthermore H and H' specify the target helicities before and after the interaction.

Lorentz covariance, parity and time reversal invariance, hermiticity and current conservation imply that the hadronic tensor of the free nucleon is expressed in terms of four structure functions F_1^N, F_2^N and g_1^N, g_2^N which depend on the momentum transfer $Q^2 = -q^2$ and $x_T = Q^2/2\nu$ with $\nu = p \cdot q$ ¹:

¹We use the notation x_T for the Bjorken variable of a target nucleus, while x denotes that of the nucleon as usual, i.e. $x = \frac{Q^2}{2Mq_0}$ in the lab frame.

$$W_{\mu\nu}^N = -g_{\mu\nu} F_1^N + \frac{p_\mu p_\nu}{\nu} F_2^N + \frac{i}{\nu} \varepsilon_{\mu\nu\lambda\sigma} q^\lambda s^\sigma g_1^N + \frac{i}{\nu^2} \varepsilon_{\mu\nu\lambda\sigma} q^\lambda (p \cdot q s^\sigma - s \cdot q p^\sigma) g_2^N. \quad (5)$$

With the nucleon helicities $H, H' = +, - = \uparrow, \downarrow$ we obtain from Eqs.(3,4,5) for the spin-averaged structure functions:

$$F_1^N = \frac{1}{4\pi e^2} \left(\text{Im} \mathcal{A}_{+\downarrow,+\downarrow}^{\gamma^*N} + \text{Im} \mathcal{A}_{+\uparrow,+\uparrow}^{\gamma^*N} \right), \quad (6a)$$

$$F_2^N = \frac{x}{2\pi e^2 \kappa_N} \left(\text{Im} \mathcal{A}_{+\downarrow,+\downarrow}^{\gamma^*N} + \text{Im} \mathcal{A}_{+\uparrow,+\uparrow}^{\gamma^*N} + 2\text{Im} \mathcal{A}_{0\uparrow,0\uparrow}^{\gamma^*N} \right), \quad (6b)$$

and for the spin-dependent ones:

$$g_1^N = \frac{1}{4\pi e^2 \kappa_N} \left(\text{Im} \mathcal{A}_{+\downarrow,+\downarrow}^{\gamma^*N} - \text{Im} \mathcal{A}_{+\uparrow,+\uparrow}^{\gamma^*N} + \sqrt{2(\kappa_N - 1)} \text{Im} \mathcal{A}_{+\downarrow,0\uparrow}^{\gamma^*N} \right), \quad (6c)$$

$$g_2^N = \frac{1}{4\pi e^2 \kappa_N} \left(\text{Im} \mathcal{A}_{+\uparrow,+\uparrow}^{\gamma^*N} - \text{Im} \mathcal{A}_{+\downarrow,+\downarrow}^{\gamma^*N} + \frac{2}{\sqrt{2(\kappa_N - 1)}} \text{Im} \mathcal{A}_{+\downarrow,0\uparrow}^{\gamma^*N} \right). \quad (6d)$$

Here $\kappa_N = 1 + M^2 Q^2 / \nu^2$ with the nucleon mass M .

For deuterium, as for any spin-1 target, the hadronic tensor has eight structure functions. Four of them are proportional to Lorentz structures as found for free nucleons (5). Of the remaining structure functions b_1, b_2, Δ and b_3 , the first three occur at leading twist while b_3 is suppressed at large Q^2 [9,11]:

$$\begin{aligned} W_{\mu\nu}^d = & -g_{\mu\nu} F_1^d + \frac{p_\mu p_\nu}{\nu} F_2^d + \frac{i}{\nu} \varepsilon_{\mu\nu\lambda\sigma} q^\lambda s^\sigma g_1^d + \frac{i}{\nu^2} \varepsilon_{\mu\nu\lambda\sigma} q^\lambda (p \cdot q s^\sigma - s \cdot q p^\sigma) g_2^d \\ & - \left(g_{\mu\nu} b_1 - \frac{p_\mu p_\nu}{\nu} b_2 \right) \left(\frac{M_d^2}{\kappa_d \nu^2} q \cdot \mathcal{E} q \cdot \mathcal{E}^* - \frac{1}{3} \right) \\ & + \frac{\Delta}{2} \left\{ \left(-g_{\mu\nu} + \frac{2x_T}{\kappa_d \nu} p_\mu p_\nu \right) \left(\frac{M_d^2}{\kappa_d \nu^2} q \cdot \mathcal{E} q \cdot \mathcal{E}^* - 1 \right) + \left[\left(\mathcal{E}_\mu - \frac{q \cdot \mathcal{E}}{\kappa_d \nu} p_\mu \right) \left(\mathcal{E}_\nu^* - \frac{q \cdot \mathcal{E}^*}{\kappa_d \nu} p_\nu \right) + (\mu \leftrightarrow \nu) \right] \right\} \\ & + b_3 \frac{\kappa_d - 1}{\sqrt{\kappa_d \nu}} \left[p_\mu q \cdot \mathcal{E}^* \left(\mathcal{E}_\nu - \frac{q \cdot \mathcal{E}}{\kappa_d \nu} p_\nu \right) + p_\mu q \cdot \mathcal{E} \left(\mathcal{E}_\nu^* - \frac{q \cdot \mathcal{E}^*}{\kappa_d \nu} p_\nu \right) + (\mu \leftrightarrow \nu) \right]. \end{aligned} \quad (7)$$

Here we use $\kappa_d = 1 + M_d^2 Q^2 / \nu^2$ and omit the spin indices H in the deuteron polarization vector \mathcal{E} . The relations between helicity amplitudes and structure functions are obtained again from Eqs.(3,4,7):

$$F_1^d = \frac{1}{6\pi e^2} \left(\text{Im} \mathcal{A}_{++;++}^{\gamma^*d} + \text{Im} \mathcal{A}_{+-;+-}^{\gamma^*d} + \text{Im} \mathcal{A}_{+0,+0}^{\gamma^*d} \right), \quad (8a)$$

$$F_2^d = \frac{x_T}{3\pi e^2 \kappa_d} \left(\text{Im} \mathcal{A}_{++;++}^{\gamma^*d} + \text{Im} \mathcal{A}_{+-;+-}^{\gamma^*d} + \text{Im} \mathcal{A}_{+0,+0}^{\gamma^*d} + 2\text{Im} \mathcal{A}_{0+,0+}^{\gamma^*d} + \text{Im} \mathcal{A}_{00,00}^{\gamma^*d} \right), \quad (8b)$$

$$g_1^d = \frac{1}{4\pi e^2 \kappa_d} \left(\text{Im} \mathcal{A}_{+-;+-}^{\gamma^*d} - \text{Im} \mathcal{A}_{++;++}^{\gamma^*d} + \sqrt{\kappa_d - 1} (\text{Im} \mathcal{A}_{+0,+0}^{\gamma^*d} + \text{Im} \mathcal{A}_{+-,00}^{\gamma^*d}) \right), \quad (8c)$$

$$g_2^d = \frac{1}{4\pi e^2 \kappa_d} \left(\text{Im} \mathcal{A}_{++;++}^{\gamma^*d} - \text{Im} \mathcal{A}_{+-;+-}^{\gamma^*d} + \frac{1}{\sqrt{\kappa_d - 1}} (\text{Im} \mathcal{A}_{+0,+0}^{\gamma^*d} + \text{Im} \mathcal{A}_{+-,00}^{\gamma^*d}) \right), \quad (8d)$$

$$b_1 = -\frac{1}{4\pi e^2} \left(\text{Im} \mathcal{A}_{++,++}^{\gamma^*d} + \text{Im} \mathcal{A}_{+,-,+}^{\gamma^*d} - 2\text{Im} \mathcal{A}_{+0,+0}^{\gamma^*d} \right), \quad (8e)$$

$$b_2 = -\frac{x_T}{2\pi e^2 \kappa_d} \left(\text{Im} \mathcal{A}_{++,++}^{\gamma^*d} + \text{Im} \mathcal{A}_{+,-,+}^{\gamma^*d} - 2\text{Im} \mathcal{A}_{+0,+0}^{\gamma^*d} + 2\text{Im} \mathcal{A}_{0+,0+}^{\gamma^*d} - 2\text{Im} \mathcal{A}_{00,00}^{\gamma^*d} \right), \quad (8f)$$

$$\Delta = \frac{1}{2\pi e^2} \text{Im} \mathcal{A}_{+,-,+}^{\gamma^*d}, \quad (8g)$$

$$b_3 = \frac{1}{4\pi e^2 \sqrt{\kappa_d(\kappa_d - 1)}} (\text{Im} \mathcal{A}_{+0,0+}^{\gamma^*d} - \text{Im} \mathcal{A}_{+-,00}^{\gamma^*d}). \quad (8h)$$

The scaling property of the structure functions (8) requires that the amplitudes $\mathcal{A}_{+0,0+}^{\gamma^*d}$ and $\mathcal{A}_{+-,00}^{\gamma^*d}$ drop at least as $1/\sqrt{Q^2}$.

III. DEEP-INELASTIC SCATTERING FROM DEUTERONS AT SMALL x

From the previous discussion we find that in the scaling limit, which we use throughout, the structure functions F_1^d, F_2^d, g_1^d and b_1 are determined by the helicity conserving amplitudes $\mathcal{A}_{+H}^{\gamma^*d} \equiv \mathcal{A}_{+H,+H}^{\gamma^*d}$. These can be split into single and double scattering parts as sketched in Fig.2:

$$\mathcal{A}_{+H}^{\gamma^*d} = \mathcal{A}_{+H}^{(1)} + \mathcal{A}_{+H}^{(2)}. \quad (9)$$

In the single scattering term the photon interacts incoherently with the proton or neutron of the target. The double scattering term involves interactions in which both nucleons take part. In the following we derive the corresponding amplitudes extending the Glauber-Gribov multiple scattering theory [20–22] to include spin degrees of freedom.

A. Single scattering

We first focus on single scattering contributions to the structure functions $F_{1(2)}^d, g_1^d$ and b_1 . The corresponding Compton amplitude reads (Fig.2a):

$$\begin{aligned} i\mathcal{A}_{+H}^{(1)} = & - \int \frac{d^4p}{(2\pi)^4} \mathcal{E}_H^{\alpha*} \varepsilon_+^{\mu*} \text{Tr} \left[\Gamma_\beta(p_d, p) \frac{i}{\not{p}_d - \not{p} - M + i\varepsilon} \bar{\Gamma}_\alpha(p_d, p) \right. \\ & \left. \times \frac{i}{\not{p} - M + i\varepsilon} i\hat{t}_{\mu\nu}^{\gamma^*p}(p, q) \frac{i}{\not{p} - M + i\varepsilon} \right] \mathcal{E}_H^\beta \varepsilon_+^\nu + [p \leftrightarrow n], \end{aligned} \quad (10)$$

We describe the scattering process in the laboratory frame where the deuteron with four-momentum $p_d^\mu = (M_d, \mathbf{0})$ is at rest. The integration in (10) runs over the momentum $p^\mu = (p^0, \mathbf{p})$ of the interacting nucleon. The polarization vectors of the transverse photon and the deuteron are denoted by ε_+ and \mathcal{E}_H , respectively. All information about deuteron structure is absorbed in the vertex functions Γ , such that the free proton and neutron propagators remain. The interaction of the photon with the bound nucleon is described by the reduced amplitude \hat{t}^{γ^*N} which is related to the physical photon-nucleon forward scattering amplitudes in (6) as follows:

$$\mathcal{A}_{+h}^{\gamma^*N} = \varepsilon_+^{\mu*} \bar{u}(p, h) \hat{t}_{\mu\nu}^{\gamma^*N}(p, q) u(p, h) \varepsilon_+^\nu. \quad (11)$$

Here $u(p, h)$ is the Dirac spinor of a nucleon with momentum p and helicity h .

One can perform the energy integration in (10) assuming that all relevant poles are included in the nucleon propagators. We neglect modifications of the individual nucleon amplitudes \mathcal{A}^{γ^*N} due to nuclear binding and Fermi motion. They are relevant only at moderate and large x (see e.g. [5,23]), whereas our primary interest in this paper is the region $x < 0.1$. Next we perform a non-relativistic expansion of the nucleon propagators in (10), keeping only the leading terms in $|\mathbf{p}|/M$. In the non-relativistic limit we identify the vertex functions Γ with non-relativistic deuteron wave functions ψ_H . We find (for details see Appendix A):

$$\mathcal{A}_{+H}^{(1)} = \int d^3r \psi_H^\dagger(\mathbf{r}) \left(P_\uparrow^p \mathcal{A}_{+\uparrow}^{\gamma^*p} + P_\downarrow^p \mathcal{A}_{+\downarrow}^{\gamma^*p} \right) \psi_H(\mathbf{r}) + [p \leftrightarrow n]. \quad (12)$$

The operators $P_{\uparrow(\downarrow)}^N$ act on the deuteron wave function and project onto a proton or neutron with helicity $+$ or $-$. The coordinate-space wave function of the deuteron is:

$$\psi_H(\mathbf{r}) = \frac{1}{\sqrt{4\pi}} \left[\frac{u(r)}{r} + \frac{v(r)}{r} \frac{1}{\sqrt{8}} \hat{S}_{12}(\hat{\mathbf{r}}) \right] \chi_H, \quad (13)$$

where $\hat{S}_{12}(\hat{\mathbf{r}}) = 3(\boldsymbol{\sigma}_p \cdot \mathbf{r})(\boldsymbol{\sigma}_n \cdot \mathbf{r})/r^2 - \boldsymbol{\sigma}_p \cdot \boldsymbol{\sigma}_n$ is the tensor operator with $r = |\mathbf{r}|$, and χ_H denotes the spin wave function of the triplet proton-neutron pair. The deuteron S - and D -state components are determined by the radial wave functions u and v , respectively. They are normalized according to $\int_0^\infty dr [u^2(r) + v^2(r)] = 1$, while the D -state probability is given by $\omega_D = \int_0^\infty dr v^2(r)$.

Inserting the deuteron wave function in Eq.(12) and working out the projection operators for the different deuteron polarizations, one finds:

$$\mathcal{A}_{++}^{(1)} = \left(1 - \frac{3}{4}\omega_D \right) (\mathcal{A}_{+\uparrow}^{\gamma^*p} + \mathcal{A}_{+\uparrow}^{\gamma^*n}) + \frac{3}{4}\omega_D (\mathcal{A}_{+\downarrow}^{\gamma^*p} + \mathcal{A}_{+\downarrow}^{\gamma^*n}), \quad (14a)$$

$$\mathcal{A}_{+-}^{(1)} = \left(1 - \frac{3}{4}\omega_D \right) (\mathcal{A}_{+\downarrow}^{\gamma^*p} + \mathcal{A}_{+\downarrow}^{\gamma^*n}) + \frac{3}{4}\omega_D (\mathcal{A}_{+\uparrow}^{\gamma^*p} + \mathcal{A}_{+\uparrow}^{\gamma^*n}), \quad (14b)$$

$$\mathcal{A}_{+0}^{(1)} = \frac{1}{2} (\mathcal{A}_{+\uparrow}^{\gamma^*p} + \mathcal{A}_{+\downarrow}^{\gamma^*p} + \mathcal{A}_{+\uparrow}^{\gamma^*n} + \mathcal{A}_{+\downarrow}^{\gamma^*n}). \quad (14c)$$

With Eqs.(6,8) the single scattering contributions to the deuteron structure functions become:

$$F_1^d = F_1^p + F_1^n = 2F_1^N, \quad (15a)$$

$$g_1^d = \left(1 - \frac{3}{2}\omega_D \right) (g_1^p + g_1^n) = (2 - 3\omega_D) g_1^N, \quad (15b)$$

$$b_1 = 0. \quad (15c)$$

We end up with the incoherent sum of the corresponding proton and neutron structure functions. The polarized structure function g_1^d includes the depolarization factor $(1 - 3\omega_D/2)$. It accounts for the fact that the deuteron and the interacting nucleon can be polarized in opposite directions if the deuteron is in a D -state. Note that b_1 vanishes for single scattering since there is no such structure function for the individual spin-1/2 particles.

B. Double scattering

At small values of the Bjorken variable, $x < 0.1$, double scattering contributes significantly to photon-deuteron Compton scattering and consequently to deuteron structure functions. In this process the virtual photon diffractively produces a hadronic intermediate state on the first nucleon, which subsequently interacts with the second nucleon. In the case of unpolarized scattering destructive interference of the single and double scattering amplitudes leads to the observed nuclear shadowing (see e.g. [24]).

The helicity dependent double scattering amplitude reads (see Fig.2b):

$$\begin{aligned}
i\mathcal{A}_{+H}^{(2)} = & - \sum_X \int \frac{d^4 p}{(2\pi)^4} \int \frac{d^4 k}{(2\pi)^4} \mathcal{E}_H^{\alpha*} \varepsilon_+^{\mu*} \frac{-i(g^{\rho\sigma} - p_X^\rho p_X^\sigma / M_X^2)}{p_X^2 - M_X^2 + i\varepsilon} \\
& \times \text{Tr} \left[\Gamma_\beta(p_d, p) \frac{i}{\not{p}_d - \not{p} - M + i\varepsilon} i \hat{t}_{\mu\rho}^{Xn \rightarrow \gamma^* n} \frac{i}{\not{p}_d - \not{p} - \not{k} - M + i\varepsilon} \bar{\Gamma}_\alpha(p_d, p) \right. \\
& \left. \times \frac{i}{\not{p} + \not{k} - M + i\varepsilon} i \hat{t}_{\sigma\nu}^{\gamma^* p \rightarrow Xp} \frac{i}{\not{p} - M + i\varepsilon} \right] \mathcal{E}_H^\beta \varepsilon_+^\nu \\
& + [p \leftrightarrow n].
\end{aligned} \tag{16}$$

Here p denotes the four-momentum of the first interacting nucleon and k the momentum transfer. The sum is taken over all diffractively excited hadronic states X which carry photon quantum numbers, an invariant mass M_X and a four-momentum $p_X = q - k$. Their contributions to double scattering are determined by the reduced amplitudes $\hat{t}^{\gamma^* N \rightarrow XN}$ which are related to the diffractive (virtual) photoproduction amplitudes of hadronic states X from nucleons by:

$$T_{+h}^{NX}(k) = \varepsilon_{X+}^{\sigma*} \bar{u}(p+k, h) \hat{t}_{\sigma\nu}^{\gamma^* N \rightarrow XN} u(p, h) \varepsilon_+^\nu, \tag{17}$$

where ε_{X+} denotes the transverse polarization vector of the produced hadronic intermediate states. We choose the photon momentum in the longitudinal direction, $q^\mu = (q_0, \mathbf{0}_\perp, \sqrt{q_0^2 + Q^2})$. As in single scattering we perform the energy integration in (16) assuming that all relevant poles are in the propagators. We then take into account only the leading non-relativistic contribution to $\mathcal{A}^{(2)}$. Furthermore we assume that the diffractive amplitudes \hat{t} depend on the transverse momentum transfer only. Following the steps given in Appendix B this leads to:

$$\begin{aligned}
\mathcal{A}_{+H}^{(2)} = & \frac{i}{4Mq_0} \sum_X \int \frac{d^2 k_\perp}{(2\pi)^2} \int d^2 b e^{i\mathbf{k}_\perp \cdot \mathbf{b}} \int_{-\infty}^0 dz e^{i\frac{z}{X}} \\
& \times \psi_H^\dagger(\mathbf{r}) \left(P_\uparrow^p T_{+\uparrow}^{pX}(k) + P_\downarrow^p T_{+\downarrow}^{pX}(k) \right) \otimes \left(P_\uparrow^n T_{+\uparrow}^{nX}(k) + P_\downarrow^n T_{+\downarrow}^{nX}(k) \right) \psi_H(\mathbf{r}) \\
& + [p \leftrightarrow n].
\end{aligned} \tag{18}$$

In analogy with hadron-hadron high-energy collisions [25] the real part of diffractive production amplitudes is supposed to be small. We therefore use in the following $T^{NX} \approx i \text{Im} T^{NX}$ and consider only terms which contribute to the imaginary part of the double scattering amplitude $\mathcal{A}^{(2)}$.

For the double scattering contribution to be significant, the longitudinal propagation length

$$\lambda \simeq \frac{2q_0}{M_X^2 + Q^2} = \frac{1}{x M} \left(\frac{Q^2}{M_X^2 + Q^2} \right) \quad (19)$$

of a diffractively excited hadron must exceed the size of the deuteron target, $d = \langle r^2 \rangle_d^{1/2} \approx 4 \text{ fm}$. At large Q^2 the important intermediate states are those with $M_X^2 \sim Q^2$ (see e.g. Refs. [21,24,26]). Hence the condition $\lambda > d$ is fulfilled for $x < 0.03$ in agreement with the observed shadowing effect in unpolarized deep-inelastic scattering [6–8].

After projecting onto proton and neutron states with definite helicity one finds:

$$\mathcal{A}_{++}^{(2)} \approx \frac{i}{4Mq_0} \sum_X \int \frac{d^2 k_\perp}{(2\pi)^2} S_+(\mathbf{k}_\perp, 1/\lambda) T_{+\uparrow}^{pX}(k) T_{+\uparrow}^{nX}(k), \quad (20a)$$

$$\mathcal{A}_{+-}^{(2)} \approx \frac{i}{4Mq_0} \sum_X \int \frac{d^2 k_\perp}{(2\pi)^2} S_-(\mathbf{k}_\perp, 1/\lambda) T_{+\downarrow}^{pX}(k) T_{+\downarrow}^{nX}(k), \quad (20b)$$

$$\mathcal{A}_{+0}^{(2)} \approx \frac{i}{8Mq_0} \sum_X \int \frac{d^2 k_\perp}{(2\pi)^2} S_0(\mathbf{k}_\perp, 1/\lambda) \left[T_{+\uparrow}^{pX}(k) T_{+\downarrow}^{nX}(k) + T_{+\downarrow}^{pX}(k) T_{+\uparrow}^{nX}(k) \right], \quad (20c)$$

with the helicity dependent deuteron form factor

$$S_H(\mathbf{k}) = \int d^3 r |\psi_H(\mathbf{r})|^2 e^{i\mathbf{k} \cdot \mathbf{r}}. \quad (21)$$

In Eq.(20) we have neglected contributions which vanish for diffractive production processes in the forward direction. At small scattering angles θ the omitted terms are suppressed by typical factors $(\sin \theta / \cos \theta)^2$. Note in addition that the neglected contributions are proportional to the square of the deuteron D -state wave function and therefore numerically insignificant in any case. The complete expressions for the helicity amplitudes $\mathcal{A}^{(2)}$ can be found in Appendix B.

For the following discussion we approximate the dependence of the diffractive production amplitudes on the momentum transfer $t = k^2 \approx -\mathbf{k}_\perp^2$ by:

$$T^{NX}(k) \approx e^{-B \mathbf{k}_\perp^2 / 2} T^{NX}. \quad (22)$$

with the forward amplitude $T^{NX} \equiv T^{NX}(\mathbf{k} = 0)$. For possible small momentum transfers an exponential suppression of T^{NX} with rising $|t|$ is certainly justified and supported by experiment [27–30]. Furthermore we finally investigate our results for deuteron spin structure functions in the kinematic range of fixed target experiments at CERN (NMC, COMPASS), FNAL (E665) and DESY (HERMES). Here in average moderate momentum transfers, $Q^2 \lesssim 3 \text{ GeV}^2$, are accessible at $x < 0.1$. Various data on diffractive leptonproduction in this kinematic region [27–30] suggest an average slope $B \simeq (6 \dots 10) \text{ GeV}^{-2}$. Note that the limit $B = 0$ corresponds to the approximation that the diffractive production of intermediate hadronic states proceeds in the forward direction, i.e. at a fixed impact parameter $\mathbf{b} = 0$ (18).

The double scattering amplitudes $\mathcal{A}^{(2)}$ can now be expressed in terms of the integrated form factors:

$$\mathcal{F}_H(1/\lambda, B) = \int \frac{d^2 k_\perp}{(2\pi)^2} S_H(\mathbf{k}_\perp, 1/\lambda) e^{-B \mathbf{k}_\perp^2}. \quad (23)$$

In Fig.3 we present \mathcal{F}_H for realistic wave functions as obtained from the Paris [31] and Bonn [32] nucleon-nucleon potentials. We observe a significant dependence on the deuteron polarization. Furthermore we find $\mathcal{F}_H \approx \text{constant}$ for $\lambda > \langle r^2 \rangle_d^{1/2} \approx 4 \text{ fm}$. To investigate the influence of the diffractive slope B we compare results for $B = 7 \text{ GeV}^{-2}$ and $B = 0$. We find that the form factors for unpolarized deuterium,

$$\mathcal{F} = \frac{1}{3} (\mathcal{F}_+ + \mathcal{F}_- + \mathcal{F}_0), \quad (24)$$

and for transverse polarization, \mathcal{F}_+ , are not very sensitive to the exact value of the diffractive slope. In the examples shown in Fig.3 they vary by maximally 15%. The situation is different for tensor polarization. For $\lambda > 4 \text{ fm}$ the corresponding form factor

$$\mathcal{F}_T = \frac{1}{2} (\mathcal{F}_+ + \mathcal{F}_- - 2\mathcal{F}_0) \quad (25)$$

increases approximately by a factor of three when $B = 0$ is chosen instead of $B = 7 \text{ GeV}^{-2}$. The reason is that the deuteron tensor form factor $S_T = S_+ + S_- - 2S_0$ receives significant contributions from rather large momenta $|\mathbf{k}| \simeq (200\text{--}400) \text{ MeV}$. In this kinematic region S_T varies slowly with $t \sim -\mathbf{k}_\perp^2$. As a consequence the forward approximation, $B = 0$, is poorly justified in this case.² In addition note that the differences between form factors derived from the Bonn and the Paris potential become small if a realistic slope is used.

Combining Eqs.(20,22,23) finally gives:

$$\mathcal{A}_{++}^{(2)} = \frac{i}{4M_{q0}} \sum_X T_{+\uparrow}^{pX} T_{+\uparrow}^{nX} \mathcal{F}_+(1/\lambda, B), \quad (26a)$$

$$\mathcal{A}_{+-}^{(2)} = \frac{i}{4M_{q0}} \sum_X T_{+\downarrow}^{pX} T_{+\downarrow}^{nX} \mathcal{F}_-(1/\lambda, B), \quad (26b)$$

$$\mathcal{A}_{+0}^{(2)} = \frac{i}{8M_{q0}} \sum_X \left(T_{+\downarrow}^{pX} T_{+\uparrow}^{nX} + T_{+\uparrow}^{pX} T_{+\downarrow}^{nX} \right) \mathcal{F}_0(1/\lambda, B). \quad (26c)$$

In combination with Eq.(8) we then obtain the double scattering corrections to all deuteron structure functions.

For the unpolarized structure function $F_1^d = F_1^p + F_1^n + \delta F_1$ we have:

$$\delta F_1 = \frac{1}{6\pi e^2} \left[\text{Im} \mathcal{A}_{++}^{(2)} + \text{Im} \mathcal{A}_{+-}^{(2)} + \text{Im} \mathcal{A}_{+0}^{(2)} \right], \quad (27)$$

$$\begin{aligned} &= \frac{1}{32\pi e^2 M_{q0}} \sum_X \left\{ \mathcal{F}(1/\lambda, B) \left(T_{+\uparrow}^{pX} T_{+\uparrow}^{pX} + T_{+\downarrow}^{pX} T_{+\downarrow}^{pX} + T_{+\uparrow}^{nX} T_{+\uparrow}^{nX} + T_{+\downarrow}^{nX} T_{+\downarrow}^{nX} \right) \right. \\ &\quad \left. - \mathcal{F}(1/\lambda, B) \left[(T_{+\uparrow}^{pX} - T_{+\uparrow}^{nX})^2 + (T_{+\downarrow}^{pX} - T_{+\downarrow}^{nX})^2 \right] \right. \\ &\quad \left. - \frac{2}{3} \mathcal{F}_0(1/\lambda, B) (T_{+\uparrow}^{pX} - T_{+\downarrow}^{pX}) (T_{+\uparrow}^{nX} - T_{+\downarrow}^{nX}) \right\}. \end{aligned} \quad (28)$$

If we ignore the isospin and spin dependent combinations proportional to

²We thank N.N. Nikolaev and M.I. Strikman for discussions related to this issue.

$$(T_{+\uparrow}^{pX} - T_{+\uparrow}^{nX})^2, (T_{+\downarrow}^{pX} - T_{+\downarrow}^{nX})^2 \text{ and } (T_{+\uparrow}^{pX} - T_{+\downarrow}^{pX})(T_{+\uparrow}^{nX} - T_{+\downarrow}^{nX}), \quad (29)$$

we arrive at the well known result [21]

$$\delta F_1 = -\frac{2Q^2}{e^2 x} \int_{4m_\pi^2}^{W^2} dM_X^2 \left(\left. \frac{d^2 \sigma_{\downarrow}^{\gamma_T^{*N}}}{dM_X^2 dt} \right|_{t=0} + \left. \frac{d^2 \sigma_{\uparrow}^{\gamma_T^{*N}}}{dM_X^2 dt} \right|_{t=0} \right) \mathcal{F}(1/\lambda, B), \quad (30)$$

written in terms of the forward diffractive hadron production cross section in the collision of transverse virtual photons with nucleons at $t = (p_X - q)^2 \approx 0$. The individual helicity dependent diffractive cross sections are:

$$16\pi \int_{4m_\pi^2}^{W^2} dM_X^2 \left. \frac{d^2 \sigma_h^{\gamma_T^{*N}}}{dM_X^2 dt} \right|_{t \approx 0} = \frac{1}{8M^2 q_0^2} \sum_X (|T_{+h}^{pX}|^2 + |T_{+h}^{nX}|^2). \quad (31)$$

In Sec.IV we investigate all terms of Eq.(28) as they contribute to δF_1 within a simple model. The corrections to the conventional result, Eq.(30), turn out to be small indeed. In Fig.4 we present the shadowing correction for the unpolarized structure function $F_2^d/2F_2^N$ as measured by the E665 collaboration [6]. At $x \ll 0.1$ one finds $\delta F_2/2F_2^N \approx \delta F_1/2F_1^N \approx -0.03$, with large experimental errors. Note however that the quoted value is consistent with an analysis of the A -dependence of nuclear shadowing in Ref. [33]. For later estimates of double scattering effects in deuteron spin structure functions we use the fit to the data shown in Fig.4. Corresponding theoretical calculations can be found for example in Ref. [34].

Following Eqs.(8,26), the double scattering to the polarized structure function $g_1^d = (1 - 3\omega_D/2)(g_1^p + g_1^n) + \delta g_1$ is:

$$\delta g_1 = \frac{1}{4\pi e^2} [Im\mathcal{A}_{+-}^{(2)} - Im\mathcal{A}_{++}^{(2)}] \quad (32)$$

$$= \frac{1}{32\pi e^2 M q_0} \sum_X \mathcal{F}_+(1/\lambda, B) [T_{+\downarrow}^{pX} T_{+\downarrow}^{pX} - T_{+\uparrow}^{pX} T_{+\uparrow}^{pX} + T_{+\downarrow}^{nX} T_{+\downarrow}^{nX} - T_{+\uparrow}^{nX} T_{+\uparrow}^{nX} + (T_{+\uparrow}^{pX} - T_{+\uparrow}^{nX})^2 - (T_{+\downarrow}^{pX} - T_{+\downarrow}^{nX})^2]. \quad (33)$$

If one assumes that spin averaged diffractive amplitudes are equal for protons and neutrons, i.e. $T_{+\uparrow}^{pX} + T_{+\downarrow}^{pX} = T_{+\uparrow}^{nX} + T_{+\downarrow}^{nX}$, the third and fourth terms in Eq.(33) vanish. In Regge phenomenology this is guaranteed by the isospin independent pomeron exchange which dominates diffraction at small x (see e.g. [35]). We then end up with:

$$\delta g_1 = -\frac{2Q^2}{e^2 x} \int_{4m_\pi^2}^{W^2} dM_X^2 \left(\left. \frac{d^2 \sigma_{\downarrow}^{\gamma_T^{*N}}}{dM_X^2 dt} \right|_{t=0} - \left. \frac{d^2 \sigma_{\uparrow}^{\gamma_T^{*N}}}{dM_X^2 dt} \right|_{t=0} \right) \mathcal{F}_+(1/\lambda, B). \quad (34)$$

Now the difference of the helicity dependent diffractive production cross sections enters, whereas the unpolarized case, Eq.(30), involves the sum of both.

Finally we study the structure function b_1 which does not receive contributions from single scattering as long as nuclear binding and Fermi motion are neglected. Here double scattering gives:

$$\begin{aligned}
b_1 &= -\frac{1}{4\pi e^2} \left(\text{Im } \mathcal{A}_{++}^{(2)} + \text{Im } \mathcal{A}_{+-}^{(2)} - 2\text{Im } \mathcal{A}_{+0}^{(2)} \right), \\
&= \frac{1}{32\pi e^2 M_{q0}} \sum_X \left\{ \mathcal{F}_0(1/\lambda, B) \left[T_{+\uparrow}^{pX} T_{+\uparrow}^{pX} + T_{+\downarrow}^{pX} T_{+\downarrow}^{pX} + T_{+\uparrow}^{nX} T_{+\uparrow}^{nX} + T_{+\downarrow}^{nX} T_{+\downarrow}^{nX} \right. \right. \\
&\quad \left. \left. - (T_{+\uparrow}^{pX} - T_{+\uparrow}^{nX})^2 - (T_{+\downarrow}^{pX} - T_{+\downarrow}^{nX})^2 \right. \right. \\
&\quad \left. \left. - 2(T_{+\uparrow}^{pX} - T_{+\downarrow}^{pX})(T_{+\uparrow}^{nX} - T_{+\downarrow}^{nX}) \right] \right. \\
&\quad \left. - \mathcal{F}_+(1/\lambda, B) \left[T_{+\uparrow}^{pX} T_{+\uparrow}^{pX} + T_{+\downarrow}^{pX} T_{+\downarrow}^{pX} + T_{+\uparrow}^{nX} T_{+\uparrow}^{nX} + T_{+\downarrow}^{nX} T_{+\downarrow}^{nX} \right. \right. \\
&\quad \left. \left. - (T_{+\uparrow}^{pX} - T_{+\uparrow}^{nX})^2 - (T_{+\downarrow}^{pX} - T_{+\downarrow}^{nX})^2 \right] \right\}.
\end{aligned} \tag{35}$$

With the approximations (29) we obtain:

$$b_1 = \frac{4Q^2}{e^2 x} \int_{4m_\pi^2}^{W^2} dM_X^2 \left. \frac{d^2 \sigma^{\gamma_T^* N}}{dM_X^2 dt} \right|_{t=0} \mathcal{F}_T(1/\lambda, B), \tag{36}$$

and observe that b_1 is proportional to the difference of the deuteron form factors (25) for transverse and longitudinal target polarizations. This contribution is entirely driven by the interference of the deuteron S - and D -state component as can be seen from Eq.(86). Note that our result in Eq.(36) implies a violation of the quark model sum rule [16]

$$\int_0^1 dx b_1(x, Q^2) = 0, \tag{37}$$

which has been discussed in Ref. [36].

IV. SHADOWING IN g_1^d

Shadowing in the deuteron spin structure function g_1^d is proportional to the difference of polarized diffractive virtual photoproduction cross sections, see Eq.(34). These quantities are not measured up to now. Nevertheless it is possible to estimate the shadowing correction δg_1 to an accuracy which is sufficient for the extraction of the neutron structure function g_1^n from recent experimental data [1,3]. In the kinematic region of current experiments it is legitimate to neglect nuclear binding and Fermi motion corrections [23]. To leading order in the shadowing correction $\delta g_1/\delta g_1^N$ one then obtains:

$$g_1^n \simeq \frac{g_1^d}{1 - \frac{3}{2}\omega_D} \left(1 - \frac{\delta g_1}{2g_1^N \left(1 - \frac{3}{2}\omega_D \right)} \right) - g_1^p. \tag{38}$$

Recent fixed target experiments find $|g_1^d| < |g_1^p|$ [1,3]. The sensitivity of g_1^n to uncertainties in the nuclear depolarization or shadowing is therefore suppressed. Note that in this respect the use of ^3He targets is expected to be less favorable [19].

A. Upper limit for shadowing in g_1^d

An upper limit for shadowing in g_1^d can be obtained by directly comparing δg_1 and δF_1 in terms of the photon-deuteron helicity amplitudes (27,32). Note that at small x

their imaginary parts have the same sign. The reason is that at $x \ll 0.1$ large values of the coherence length are relevant (see Eq.(19)). For $\lambda > 4 fm$ the longitudinal deuteron form factors (23) which enter in Eq.(26) are all positive. We can then apply the Schwartz inequality

$$\left| Im\mathcal{A}_{++}^{(2)} + Im\mathcal{A}_{+-}^{(2)} + Im\mathcal{A}_{+0}^{(2)} \right| \geq \left| Im\mathcal{A}_{++}^{(2)} + Im\mathcal{A}_{+-}^{(2)} \right| \geq \left| Im\mathcal{A}_{+-}^{(2)} - Im\mathcal{A}_{++}^{(2)} \right|, \quad (39)$$

and obtain:

$$\frac{|\delta g_1|}{F_1^N} \leq \frac{3}{2} \frac{|\delta F_1|}{F_1^N} \approx \frac{3}{2} \frac{|\delta F_2|}{F_2^N}. \quad (40)$$

Given the E665 data on $F_2^d/2F_2^N$ shown in Fig.4 we conclude from Eqs.(38,40) that uncertainties due to the shadowing correction δg_1 are small. They are within the experimental errors of recent data analyses [1,3]. However, once accurate data for g_1^d and g_1^p become available at $x < 0.01$ the upper bound (40) is not helpful anymore due to the strong rise of F_1^N at small x (see e.g. [37]).

B. Model calculation

In this section we investigate double scattering contributions to deuteron structure functions in the framework of a simple model. In a laboratory frame description of deep-inelastic scattering at small $x \ll 0.1$, the exchanged virtual photon first converts to a hadronic state X which then interacts with the target. In this kinematic region the photon-nucleon helicity amplitudes $\mathcal{A}_{+h}^{\gamma^*N}$ can be described by hadron-nucleon amplitudes averaged over all hadronic states present in the photon wave function. Here hadronic states with invariant mass $M_X^2 \sim Q^2$ dominate as one can find from a spectral analysis of photon-nucleon amplitudes (e.g. [21,24,26]). We therefore approximate the photon-nucleon helicity amplitudes by effective hadron-nucleon amplitudes $\bar{\mathcal{A}}_{+h}^{XN}$ which depend weakly on kinematic parameters, times a factor which incorporates the leading Q^2 -dependence:

$$\mathcal{A}_{+h}^{\gamma^*N} \approx e^2 \frac{C(Q^2, x)}{Q^2} \bar{\mathcal{A}}_{+h}^{XN} \quad (41)$$

In the case of unpolarized scattering an effective hadron-nucleon cross section $\bar{\sigma}^{XN} = \frac{1}{2M_{q0}} Im \bar{\mathcal{A}}^{XN} \approx 17 mb$ reproduces the measured shadowing in the nuclear structure functions F_2^A [19]. Furthermore one finds, that in the kinematic domain of current fixed target experiments, the function $C(Q^2, x)$ depends only weakly on Q^2 and x [24,26], while the factor $1/Q^2$ ensures scaling of deep-inelastic structure functions as can be seen from Eqs.(42,43).

Replacing the amplitudes (6) by the effective ones of Eq.(41) yields for the nucleon structure functions:

$$F_1^N = \frac{C}{4\pi Q^2} \left(Im \bar{\mathcal{A}}_{+\downarrow}^{XN} + Im \bar{\mathcal{A}}_{+\uparrow}^{XN} \right), \quad (42a)$$

$$g_1^N = \frac{C}{4\pi Q^2} \left(Im \bar{\mathcal{A}}_{+\downarrow}^{XN} - Im \bar{\mathcal{A}}_{+\uparrow}^{XN} \right). \quad (42b)$$

The deuteron structure functions (8) are expressed in a similar way in terms of effective hadron-deuteron amplitudes:

$$F_1^d = \frac{C}{6\pi Q^2} \left(\text{Im} \bar{\mathcal{A}}_{++}^{Xd} + \text{Im} \bar{\mathcal{A}}_{+-}^{Xd} + \text{Im} \bar{\mathcal{A}}_{+0}^{Xd} \right), \quad (43a)$$

$$g_1^d = \frac{C}{4\pi Q^2} \left(\text{Im} \bar{\mathcal{A}}_{+-}^{Xd} + \text{Im} \bar{\mathcal{A}}_{++}^{Xd} \right), \quad (43b)$$

$$b_1 = -\frac{C}{4\pi Q^2} \left(\text{Im} \bar{\mathcal{A}}_{++}^{Xd} + \text{Im} \bar{\mathcal{A}}_{+-}^{Xd} - 2\text{Im} \bar{\mathcal{A}}_{+0}^{Xd} \right). \quad (43c)$$

The next step is to express the deuteron amplitudes $\bar{\mathcal{A}}^{Xd}$ in terms of nucleon amplitudes. For the double scattering contributions the corresponding relations are identical to those of Eq.(26), if one substitutes the diffractive amplitudes T^{NX} by $\bar{\mathcal{A}}^{XN}$. Using Eqs.(42) we obtain:

$$\delta F_1(x, Q^2) = \frac{-\pi x}{C(Q^2, x)} \left[\mathcal{F}(1/\lambda, B) F_1^N(x, Q^2)^2 + \frac{1}{3} (2\mathcal{F}_+(1/\lambda, B) - \mathcal{F}_0(1/\lambda, B)) g_1^p(x, Q^2) g_1^n(x, Q^2) \right], \quad (44a)$$

$$\delta g_1(x, Q^2) = \frac{-2\pi x}{C(Q^2, x)} \mathcal{F}_+(1/\lambda, B) F_1^N(x, Q^2) g_1^N(x, Q^2), \quad (44b)$$

$$b_1(x, Q^2) = \frac{\pi x}{C(Q^2, x)} \left[\mathcal{F}_T(1/\lambda, B) F_1^N(x, Q^2)^2 + (\mathcal{F}_+(1/\lambda, B) + \mathcal{F}_0(1/\lambda, B)) g_1^p(x, Q^2) g_1^n(x, Q^2) \right], \quad (44c)$$

with $\lambda \approx 1/2Mx$. In Eqs.(44a,44c) the spin and isospin combinations (29) turn out to be proportional to the product of the proton and neutron spin structure functions g_1 . In the kinematic range of current fixed target experiments they amount to less than 5% of the dominant contribution to δF_1 and b_1 , the one is proportional to the square of the unpolarized nucleon structure function F_1^N . As a consequence the standard expression for shadowing (30) and Eq.(36) for b_1 at small x seem to be good approximations.

A comparison of shadowing for unpolarized and polarized structure functions in Eqs.(44) gives:

$$\frac{\delta g_1}{g_1^N} \approx \mathcal{R}_{g_1} \frac{\delta F_1}{F_1^N} \approx \mathcal{R}_{g_1} \frac{\delta F_2}{F_2^N}, \quad \text{with} \quad \mathcal{R}_{g_1} = 2 \frac{\mathcal{F}_+(2Mx, B)}{\mathcal{F}(2Mx, B)}. \quad (45)$$

At small x and $B = 7 \text{ GeV}^{-2}$ we find $\mathcal{R}_{g_1} = 2.2$ for both, the Paris and Bonn nucleon-nucleon potentials [31,32]. (In the forward approximation, i.e. $B = 0$, one has $\mathcal{R}_{g_1} = 2.7$ for the Paris, and $\mathcal{R}_{g_1} = 2.4$ for the Bonn potential.) In Fig.5 we present the ratio $\delta g_1/g_1^N$ using the measured $F_2^d/2F_2^N$ from Fig.4 [6]. One should note that as x decreases the data for the shadowing ratio $F_2^d/2F_2^N$ are taken at decreasing values of the average momentum transfer \bar{Q}^2 [6]. Therefore our results for $\delta g_1/g_1^N$ shown in Fig.5 correspond, strictly speaking, to the fixed target kinematics of E665 [6] which is not far from the kinematics of SMC [1]. From Eq.(38) we finally find that the shadowing correction amounts to less than 5% of the experimental error on g_1^n for the SMC [1] and E143 [3] data analysis.

V. THE TENSOR STRUCTURE FUNCTION b_1 AT SMALL x

The shadowing correction δF_1 for the unpolarized structure function and the deuteron tensor structure function b_1 are directly related. At $x \ll 0.1$ the propagation lengths (19) of diffractively excited hadrons which dominate double scattering exceed the deuteron size $\lambda > \langle r^2 \rangle_d^{1/2} \approx 4 fm$. Here, as shown in Fig.3, the deuteron form factors saturate, i.e. $\mathcal{F}_H(1/\lambda < 0.25 fm^{-1}, B) \approx \mathcal{F}_H(0, B)$. A comparison of Eqs.(30) and (36) then gives:

$$b_1 = \mathcal{R}_{b_1} \delta F_1, \quad \text{with} \quad \mathcal{R}_{b_1} = -\frac{\mathcal{F}_T(0, B)}{\mathcal{F}(0, B)}. \quad (46)$$

Using $B = 7 GeV^{-2}$ we obtain from the Paris nucleon-nucleon potential [31] $\mathcal{R}_{b_1} = -0.33$, while the Bonn one-boson-exchange potential [32] gives $\mathcal{R}_{b_1} = -0.29$. A variation of the diffractive slope B by 30% leads to a change of the ratio \mathcal{R}_{b_1} by maximally 20%. In Fig.6 we present b_1 as obtained from Eq.(46), using the fit for $F_2^d/2F_2^N$ from Fig.4, together with the empirical information on F_1^N [38,39].

For the ratio of structure functions b_1/F_1^d , which is given by an asymmetry of inclusive polarized deuteron cross sections, $\sigma_{+H}^{\gamma^*d} \sim Im \mathcal{A}_{+H}^{\gamma^*d}$, we find (8):

$$\frac{b_1}{F_1^d} = -\frac{3}{2} \frac{\sigma_{++}^{\gamma^*d} + \sigma_{+-}^{\gamma^*d} - 2\sigma_{+0}^{\gamma^*d}}{\sigma_{++}^{\gamma^*d} + \sigma_{+-}^{\gamma^*d} + \sigma_{+0}^{\gamma^*d}} \approx \mathcal{R}_{b_1} \frac{\delta F_1}{2F_1^N} \approx 0.01, \quad (47)$$

i.e. b_1 amounts to around 1% of the unpolarized deuteron structure function F_1^d or, equivalently, to 2% of F_1^N . This result agrees with an early estimate in Ref. [18]. Note that the result shown here corresponds again to the kinematics of E665 [6]. It is therefore relevant with regard to possible future experiments at HERMES [12] and eventual COMPASS [40].

VI. SUMMARY

We have studied nuclear effects in the polarized deuteron structure functions g_1^d and b_1 at small values of the Bjorken variable, $x < 0.1$, where the diffractive photo-excitation of hadronic states on a target nucleon and their subsequent interaction with the second nucleon becomes important. In order to describe these coherent double scattering processes in polarized deep-inelastic scattering we have extended the Glauber-Gribov multiple scattering theory by including spin degrees of freedom. We find that shadowing effects in g_1^d are by a factor two larger than those for the unpolarized structure function F_2^d . Nevertheless they are of minor importance for the extraction of the neutron structure function g_1^n from current data on g_1^d . In this respect deuterium seems to be a more favorable target than 3He .

We observe that b_1 at small x receives large contributions from coherent double scattering. They come from an interference of the S - and D -state components of the deuteron wave function and break the simple quark model sum rule which suggests a vanishing first moment of b_1 . At $x < 0.1$, the magnitude of b_1 reaches around 2% of the unpolarized structure function F_1^N .

ACKNOWLEDGMENTS

We would like to thank N.N. Nikolaev, M. Sargsian and M.I. Strikman for helpful comments and discussions. This work was supported in part by BMBF.

VII. APPENDIX

Here we outline the derivation of the single and double scattering amplitudes (Eqs.(12,18)) in Sec.III. For this purpose we extend the Glauber-Gribov multiple scattering theory [20–22] to include spin degrees of freedom.

A. Single Scattering

We start out from the single scattering Compton amplitude in Eq.(10):

$$i\mathcal{A}_{+H}^{(1)} = - \int \frac{d^4p}{(2\pi)^4} \mathcal{E}_H^{\alpha*} \varepsilon_+^{\mu*} Tr \left[\Gamma_\beta(p_d, p) \frac{i}{\not{p}_d - \not{p} - M + i\varepsilon} \bar{\Gamma}_\alpha(p_d, p) \right. \\ \left. \times \frac{i}{\not{p} - M + i\varepsilon} i\hat{t}_{\mu\nu}^{\gamma*p}(p, q) \frac{i}{\not{p} - M + i\varepsilon} \right] \mathcal{E}_H^\beta \varepsilon_+^\nu + [p \leftrightarrow n], \quad (48)$$

where Γ refers to the dpn-vertex and \hat{t} is the reduced amplitude defined in Eq.(11). In the laboratory frame which we use throughout, the deuteron four-momentum is:

$$p_d^\mu = (M_d, \mathbf{0}) = (2(M - B), \mathbf{0}), \quad (49)$$

where B denotes the deuteron binding energy per nucleon. We perform the energy integration in Eq.(48) assuming that all relevant poles are given by the nucleon propagators. Neglecting anti-nucleon degrees of freedom this leads to the replacement:

$$\frac{1}{(p_d - p)^2 - M^2 + i\varepsilon} \rightarrow -i\pi \frac{\delta(p_d^0 - p^0 - E_p)}{E_p}, \quad (50)$$

with $E_p = \sqrt{M^2 + \mathbf{p}^2}$. We then arrive at:

$$\mathcal{A}_{+H}^{(1)} = \int \frac{d^3p}{(2\pi)^3 2E_p} \frac{\mathcal{E}_H^{\alpha*} \varepsilon_+^{\mu*} Tr[\dots] \mathcal{E}_H^\beta \varepsilon_+^\nu}{(p^2 - M^2 + i\varepsilon)^2} \Big|_{p_d^0 - p^0 = E_p} + [p \leftrightarrow n], \quad (51)$$

with

$$Tr[\dots] = Tr \left[\Gamma_\beta (\not{p}_d - \not{p} + M) \bar{\Gamma}_\alpha (\not{p} + M) \hat{t}_{\mu\nu}^{\gamma*p}(p, q) (\not{p} + M) \right]. \quad (52)$$

In the numerator of Eq.(51) we neglect terms of order \mathbf{p}^2/M^2 and replace $\not{p} + M \approx \sum_h u(p, h) \bar{u}(p, h)$ etc. in Eq.(52), where $u(p, h)$ is the Dirac spinor of a nucleon with momentum p and helicity h . This gives:

$$Tr[\dots] \approx \sum_{h, h', h''} Tr \left[\Gamma_\beta u(p_d - p, h') \bar{u}(p_d - p, h') \bar{\Gamma}_\alpha u(p, h'') \bar{u}(p, h'') \hat{t}_{\mu\nu}^{\gamma*p}(p, q) u(p, h) \bar{u}(p, h) \right]. \quad (53)$$

Next we apply helicity conservation and introduce the photon-nucleon amplitude as in Eq.(11):

$$\varepsilon_+^{\mu*} Tr[\dots] \varepsilon_+^\nu \approx \sum_{h, h'} Tr \left[\Gamma_\beta u(p_d - p, h') \bar{u}(p_d - p, h') \bar{\Gamma}_\alpha u(p, h) \bar{u}(p, h) \mathcal{A}_{+h}^{\gamma*p} \right]. \quad (54)$$

We then expand the nucleon Dirac spinors in $|\mathbf{p}|/M$ and keep the leading terms, e.g.

$$u(p, h) = \sqrt{E_p + M} \begin{pmatrix} \chi_h \\ \frac{\boldsymbol{\sigma} \cdot \mathbf{p}}{E_p + M} \chi_h \end{pmatrix} \approx \sqrt{2M} \begin{pmatrix} \chi_h \\ 0 \end{pmatrix}, \quad (55)$$

with the nucleon Pauli spinors $\chi_\uparrow = \begin{pmatrix} 1 \\ 0 \end{pmatrix}$ and $\chi_\downarrow = \begin{pmatrix} 0 \\ 1 \end{pmatrix}$. After decomposing the vertex function

$$\Gamma_\beta = \begin{pmatrix} \Gamma_\beta^A & \Gamma_\beta^B \\ \Gamma_\beta^C & \Gamma_\beta^D \end{pmatrix}, \quad (56)$$

we find for the leading non-relativistic term:

$$\varepsilon_+^{\mu*} Tr[\dots] \varepsilon_+^\nu \approx (2M)^2 \sum_{h, h'} tr \left[\Gamma_\beta^A \chi_{h'} \chi_h^\dagger \Gamma_\alpha^{A\dagger} \chi_h \chi_h^\dagger \mathcal{A}_{+h}^{\gamma*p} \right], \quad (57)$$

where the trace is taken in the 2×2 spin-space.

We also expand the denominator in Eq.(51) and use in leading non-relativistic order:

$$\frac{1}{2E_p(p^2 - M^2)^2} \approx \frac{1}{32M^3 \left(B + \frac{\mathbf{p}^2}{2M}\right)^2}. \quad (58)$$

Combined with Eq.(57) we obtain:

$$\mathcal{A}_{+H}^{(1)} = \frac{1}{8M} \int \frac{d^3p}{(2\pi)^3} \frac{\mathcal{E}_H^{*\alpha} \mathcal{E}_H^\beta}{\left(B + \frac{\mathbf{p}^2}{2M}\right)^2} \sum_{h, h'} tr \left[\Gamma_\beta^A \chi_{h'} \chi_h^\dagger \Gamma_\alpha^{A\dagger} \chi_h \chi_h^\dagger \mathcal{A}_{+h}^{\gamma*p} \right] + [p \leftrightarrow n]. \quad (59)$$

We now specify the non-relativistic deuteron wave-function with helicity H . For a spectator nucleon (here neutron) with helicity h' we find:

$$\psi_{H, h'}^\dagger(\mathbf{p}) = \frac{\chi_{h'}^\dagger \mathcal{E}_H^{*\alpha} \Gamma_\alpha^{A\dagger}}{\sqrt{8M} \left(B + \frac{\mathbf{p}^2}{2M}\right)}, \quad (60)$$

$$\psi_{H, h'}(\mathbf{p}) = \frac{\Gamma_\beta^A \mathcal{E}_H^\beta \chi_{h'}}{\sqrt{8M} \left(B + \frac{\mathbf{p}^2}{2M}\right)}. \quad (61)$$

In Eq.(59) one can express the sum over the proton helicities using helicity projection operators:

$$\begin{aligned} \sum_h \chi_h \chi_h^\dagger \mathcal{A}_{+h}^{\gamma*p} &= \chi_\uparrow \chi_\uparrow^\dagger \mathcal{A}_{+\uparrow}^{\gamma*p} + \chi_\downarrow \chi_\downarrow^\dagger \mathcal{A}_{+\downarrow}^{\gamma*p} = \begin{pmatrix} 1 & 0 \\ 0 & 0 \end{pmatrix} \mathcal{A}_{+\uparrow}^{\gamma*p} + \begin{pmatrix} 0 & 0 \\ 0 & 1 \end{pmatrix} \mathcal{A}_{+\downarrow}^{\gamma*p} \\ &= P_\uparrow^p \mathcal{A}_{+\uparrow}^{\gamma*p} + P_\downarrow^p \mathcal{A}_{+\downarrow}^{\gamma*p}. \end{aligned} \quad (62)$$

This gives:

$$\mathcal{A}_{+H}^{(1)} = \int \frac{d^3p}{(2\pi)^3} \sum_{h'} tr \left[\psi_{H, h'}(\mathbf{p}) \psi_{H, h'}^\dagger(\mathbf{p}) \left(P_\uparrow^p \mathcal{A}_{+\uparrow}^{\gamma*p} + P_\downarrow^p \mathcal{A}_{+\downarrow}^{\gamma*p} \right) \right] + [p \leftrightarrow n]. \quad (63)$$

Summing over the neutron helicities and introducing the coordinate-space wave functions (13), this finally leads to:

$$\begin{aligned}\mathcal{A}_{+H}^{(1)} &= \int \frac{d^3 p}{(2\pi)^3} \int d^3 r' e^{i\mathbf{p}\cdot\mathbf{r}'} \int d^3 r e^{-i\mathbf{p}\cdot\mathbf{r}} \psi_H^\dagger(\mathbf{r}') \left(P_\uparrow^p \mathcal{A}_{+\uparrow}^{\gamma^* p} + P_\downarrow^p \mathcal{A}_{+\downarrow}^{\gamma^* p} \right) \psi_H(\mathbf{r}) + [p \leftrightarrow n], \\ &= \int d^3 r \psi_H^\dagger(\mathbf{r}) \left(P_\uparrow^p \mathcal{A}_{+\uparrow}^{\gamma^* p} + P_\downarrow^p \mathcal{A}_{+\downarrow}^{\gamma^* p} \right) \psi_H(\mathbf{r}) + [p \leftrightarrow n].\end{aligned}\quad (64)$$

B. Double scattering

Here we start from the double scattering amplitude of Eq.(16):

$$\begin{aligned}i\mathcal{A}_{+H}^{(2)} &= - \sum_X \int \frac{d^4 p}{(2\pi)^4} \int \frac{d^4 k}{(2\pi)^4} \mathcal{E}_H^{\alpha*} \varepsilon_+^{\mu*} \frac{-i(g^{\rho\sigma} - p_X^\rho p_X^\sigma / M_X^2)}{p_X^2 - M_X^2 + i\varepsilon} \\ &\quad \times Tr \left[\Gamma_\beta(p_d, p) \frac{i}{\not{p}_d - \not{p} - M + i\varepsilon} i \hat{t}_{\mu\rho}^{Xn \rightarrow \gamma^* n} \frac{i}{\not{p}_d - \not{p} - \not{k} - M + i\varepsilon} \bar{\Gamma}_\alpha(p_d, p) \right. \\ &\quad \times \left. \frac{i}{\not{p} + \not{k} - M + i\varepsilon} i \hat{t}_{\sigma\nu}^{\gamma^* p \rightarrow Xp} \frac{i}{\not{p} - M + i\varepsilon} \right] \mathcal{E}_H^\beta \varepsilon_+^\nu \\ &\quad + [p \leftrightarrow n],\end{aligned}\quad (65)$$

with the reduced diffractive production amplitudes \hat{t} as specified in Eq.(17). As in the single scattering case we perform the energy integration assuming that all relevant poles are in the nucleon propagators. Picking up the positive energy poles this is equivalent to the replacements:

$$\frac{1}{(p_d - p)^2 - M^2 + i\varepsilon} \rightarrow -i\pi \frac{\delta(p_d^0 - p^0 - E_p)}{E_p}, \quad (66)$$

$$\frac{1}{(p + k)^2 - M^2 + i\varepsilon} \rightarrow -i\pi \frac{\delta(p^0 + k^0 - E_{p+k})}{E_{p+k}}, \quad (67)$$

with $E_{p+k} = \sqrt{M^2 + (\mathbf{p} + \mathbf{k})^2}$. We then obtain:

$$\begin{aligned}\mathcal{A}_{+H}^{(2)} &= - \sum_X \int \frac{d^3 p}{(2\pi)^3 2E_p} \int \frac{d^3 k}{(2\pi)^3 2E_{p+k}} \frac{(-g^{\rho\sigma} + p_X^\rho p_X^\sigma / M_X^2)}{p_X^2 - M_X^2 + i\varepsilon} \\ &\quad \times \frac{\mathcal{E}_H^{\alpha*} \varepsilon_+^{\mu*} Tr[...] \mathcal{E}_H^\beta \varepsilon_+^\nu}{(p^2 - M^2 + i\varepsilon)((p_d - p - k)^2 - M^2 + i\varepsilon)} \Big|_{p_d^0 - p^0 = E_p; p^0 + k^0 = E_{p+k}} \\ &\quad + [p \leftrightarrow n],\end{aligned}\quad (68)$$

with:

$$Tr[...] = Tr \left[\Gamma_\beta (\not{p}_d - \not{p} + M) \hat{t}_{\mu\rho}^{Xn \rightarrow \gamma^* n} (\not{p}_d - \not{p} - \not{k} + M) \bar{\Gamma}_\alpha (\not{p} + \not{k} + M) \hat{t}_{\sigma\nu}^{\gamma^* p \rightarrow Xp} (\not{p} + M) \right]. \quad (69)$$

In the numerator we neglect again terms of order \mathbf{p}^2/M^2 and replace $\not{p} + M \approx \sum_h u(p, h) \bar{u}(p, h)$ etc. This leads to:

$$Tr[...] \approx \sum_{h,h'} Tr \left[\Gamma_\beta u(p_d - p, h') t_{\mu\rho}^{Xn \rightarrow \gamma^* n}(k, h') \bar{u}(p_d - p - k, h') \right. \\ \left. \times \bar{\Gamma}_\alpha u(p + k, h) t_{\sigma\nu}^{\gamma^* p \rightarrow Xp}(k, h) \bar{u}(p, h) \right]. \quad (70)$$

Here we have assumed s-channel helicity conservation for high-energy diffraction. The corresponding amplitudes are:

$$t_{\sigma\nu}^{\gamma^* N \rightarrow XN}(k, h) = \bar{u}(p + k, h) \hat{t}_{\sigma\nu}^{\gamma^* N \rightarrow XN} u(p, h). \quad (71)$$

They are related to diffractive (virtual) photoproduction amplitudes by:

$$T_{+h}^{NX}(k) = \varepsilon_{X+}^{\sigma*} t_{\sigma\nu}^{\gamma^* N \rightarrow XN}(k, h) \varepsilon_+^\nu, \quad (72)$$

with ε_{X+} , the transverse polarization vector of the produced hadron. Expanding the Dirac spinors in Eq.(70) following Eq.(55) we arrive at:

$$Tr[...] \approx (2M)^2 \sum_{h,h'} tr \left[\Gamma_\beta^A \chi_{h'} t_{\mu\rho}^{Xn \rightarrow \gamma^* n}(k, h') \chi_{h'}^\dagger \Gamma_\alpha^{A\dagger} \chi_h t_{\sigma\nu}^{\gamma^* p \rightarrow Xp}(k, h) \chi_h^\dagger \right]. \quad (73)$$

When taking also the energy denominators in the leading order non-relativistic limit, i.e.

$$\frac{1}{2E_p(p^2 - M^2)} \approx \frac{1}{-8M^2(B + \frac{\mathbf{p}^2}{2M})}, \quad (74)$$

$$\frac{1}{2E_{p+k}((p_d - p - k)^2 - M^2)} \approx \frac{1}{-8M^2(B + \frac{(\mathbf{p}+\mathbf{k})^2}{2M})}, \quad (75)$$

we can again identify the non-relativistic deuteron wave-functions. For a deuteron with helicity H and a re-scattering nucleon (here neutron) with polarization h' we have:

$$\psi_{H,h'}^\dagger(\mathbf{p} + \mathbf{k}) = \frac{\chi_{h'}^\dagger \mathcal{E}_H^{\alpha*} \Gamma_\alpha^{A\dagger}}{\sqrt{8M} \left(B + \frac{(\mathbf{p}+\mathbf{k})^2}{2M} \right)}, \quad (76)$$

$$\psi_{H,h'}(\mathbf{p}) = \frac{\Gamma_\beta^A \mathcal{E}_H^\beta \chi_{h'}}{\sqrt{8M} \left(B + \frac{\mathbf{p}^2}{2M} \right)}. \quad (77)$$

In terms of coordinate-space wave functions we find:

$$\mathcal{A}_{+H}^{(2)} = -\frac{1}{2M} \sum_X \int \frac{d^3 p}{(2\pi)^3} \int \frac{d^3 k}{(2\pi)^3} \int d^3 r' e^{i(\mathbf{p}+\mathbf{k}) \cdot \mathbf{r}'} \int d^3 r e^{-i\mathbf{p} \cdot \mathbf{r}} \frac{(-g^{\rho\sigma} + p_X^\rho p_X^\sigma / M_X^2)}{p_X^2 - M_X^2 + i\varepsilon} \\ \times \mathcal{E}_H^{\alpha*} \varepsilon_+^{\mu*} \sum_{h,h'} tr \left[\psi_{H,h'}(\mathbf{r}) t_{\mu\rho}^{Xn \rightarrow \gamma^* n}(k, h') \psi_{H,h'}^\dagger(\mathbf{r}') \chi_h t_{\sigma\nu}^{\gamma^* p \rightarrow Xp}(k, h) \chi_h^\dagger \right] \mathcal{E}_H^\beta \varepsilon_+^\nu \\ + [p \leftrightarrow n]. \quad (78)$$

Neglecting the dependence of the diffractive amplitudes $t^{\gamma^* N \rightarrow XN}$ on the longitudinal momentum transfer k_z , we perform the k_z -integration, using $p_X = q - k$ and $q^\mu = (q_0, \mathbf{0}_\perp, q_z = \sqrt{q_0^2 + Q^2})$:

$$\begin{aligned} \int_{-\infty}^{\infty} dk_z \frac{e^{ik_z z}}{p_X^2 - M_X^2 + i\varepsilon} &= \int_{-\infty}^{\infty} dk_z \frac{e^{ik_z z}}{(q_0 - k_0)^2 - (q_z - k_z)^2 - \mathbf{k}_{\perp}^2 - M_X^2 + i\varepsilon}, \\ &\approx \Theta(-z) \frac{-i\pi}{q_0} e^{i\frac{z}{\lambda}} + \Theta(z) \frac{-i\pi}{q_0} e^{i(2q_z z - \frac{z}{\lambda})}. \end{aligned} \quad (79)$$

Here we neglect terms proportional to the energy transfer k_0 and to the transverse momentum transfer \mathbf{k}_{\perp} which are suppressed by the deuteron wave function in (78). Furthermore we have introduced the coherence length

$$\lambda \approx \frac{2q_0}{M_X^2 + Q^2}. \quad (80)$$

Now we make use of the completeness relation for the diffractively produced states:

$$-g^{\rho\sigma} + p_X^{\rho} p_X^{\sigma} / M_X^2 = \sum_{\lambda} \varepsilon_{X\lambda}^{\rho} \varepsilon_{X\lambda}^{\sigma*}, \quad (81)$$

and insert the diffractive amplitudes (72):

$$\begin{aligned} \mathcal{A}_{+H}^{(2)} &= \frac{i}{4Mq_0} \sum_X \int \frac{d^2 k_{\perp}}{(2\pi)^2} \int d^2 b e^{i\mathbf{k}_{\perp} \cdot \mathbf{b}} \int_{-\infty}^0 dz e^{i\frac{z}{\lambda}} \\ &\quad \times \sum_{h,h'} \text{tr} \left[\psi_{H,h'}(\mathbf{r}) T_{+h'}^{nX}(k) \psi_{H,h'}^{\dagger}(\mathbf{r}) \chi_h T_{+h}^{pX}(k) \chi_h^{\dagger} \right] \\ &\quad + [p \leftrightarrow n]. \end{aligned} \quad (82)$$

We have omitted the second term in Eq.(79) which vanishes for large photon energies. Expressed in terms of helicity projection operators we find:

$$\begin{aligned} \mathcal{A}_{+H}^{(2)} &= \frac{i}{4Mq_0} \sum_X \int \frac{d^2 k_{\perp}}{(2\pi)^2} \int d^2 b e^{i\mathbf{k}_{\perp} \cdot \mathbf{b}} \int_{-\infty}^0 dz e^{i\frac{z}{\lambda}} \frac{1}{r^2} \\ &\quad \times \psi_H^{\dagger}(\mathbf{r}) \left(P_{\uparrow}^p T_{\uparrow\uparrow}^{pX}(k) + P_{\downarrow}^p T_{\uparrow\downarrow}^{pX}(k) \right) \otimes \left(P_{\uparrow}^n T_{\uparrow\uparrow}^{nX}(k) + P_{\downarrow}^n T_{\uparrow\downarrow}^{nX}(k) \right) \psi_H(\mathbf{r}) \\ &\quad + [p \leftrightarrow n], \end{aligned} \quad (83)$$

where \otimes indicates a product of matrices operating independently on the proton and the neutron. In terms of the deuteron wave function (13) one obtains for the helicity dependent amplitudes:

$$\begin{aligned} \mathcal{A}_{++} &= \frac{i}{4Mq_0} \sum_X \int \frac{d^2 k_{\perp}}{(2\pi)^2} \int d^2 b e^{i\mathbf{k}_{\perp} \cdot \mathbf{b}} \int_{-\infty}^0 dz e^{i\frac{z}{\lambda}} \frac{1}{r^2} \\ &\quad \times \left\{ \left[u^2 |Y_{00}|^2 + uv \frac{1}{\sqrt{10}} (Y_{00}^* Y_{20} + c.c.) + v^2 \frac{1}{10} |Y_{20}|^2 \right] T_{\uparrow\uparrow}^{pX}(k) T_{\uparrow\uparrow}^{nX}(k) \right. \\ &\quad \left. + v^2 \frac{3}{20} |Y_{21}|^2 \left[T_{\uparrow\uparrow}^{pX}(k) T_{\uparrow\downarrow}^{nX}(k) + T_{\uparrow\downarrow}^{pX}(k) T_{\uparrow\uparrow}^{nX}(k) \right] + v^2 \frac{3}{5} |Y_{22}|^2 T_{\uparrow\downarrow}^{pX}(k) T_{\uparrow\downarrow}^{nX}(k) \right\}, \end{aligned} \quad (84a)$$

$$\begin{aligned} \mathcal{A}_{+-} &= \frac{i}{4Mq_0} \sum_X \int \frac{d^2 k_{\perp}}{(2\pi)^2} \int d^2 b e^{i\mathbf{k}_{\perp} \cdot \mathbf{b}} \int_{-\infty}^0 dz e^{i\frac{z}{\lambda}} \frac{1}{r^2} \\ &\quad \times \left\{ \left[u^2 |Y_{00}|^2 + uv \frac{1}{\sqrt{10}} (Y_{00}^* Y_{20} + c.c.) + v^2 \frac{1}{10} |Y_{20}|^2 \right] T_{\uparrow\downarrow}^{pX}(k) T_{\uparrow\downarrow}^{nX}(k) \right. \end{aligned}$$

$$\begin{aligned}
& +v^2 \frac{3}{20} |Y_{21}|^2 \left[T_{+\uparrow}^{pX}(k) T_{+\downarrow}^{nX}(k) + T_{+\downarrow}^{pX}(k) T_{+\uparrow}^{nX}(k) \right] + v^2 \frac{3}{5} |Y_{22}|^2 T_{+\uparrow}^{pX}(k) T_{+\uparrow}^{nX}(k) \Big\}, \quad (84b) \\
\mathcal{A}_{+0} = & \frac{i}{4M_{q0}} \sum_X \int \frac{d^2 k_\perp}{(2\pi)^2} \int d^2 b e^{i\mathbf{k}_\perp \cdot \mathbf{b}} \int_{-\infty}^0 dz e^{i\frac{z}{\lambda}} \frac{1}{2\mathbf{r}^2} \\
& \times \left\{ \left[u^2 |Y_{00}|^2 - uv \frac{2}{\sqrt{10}} (Y_{00}^* Y_{20} + c.c.) + v^2 \frac{2}{5} |Y_{20}|^2 \right] \left[T_{+\uparrow}^{pX}(k) T_{+\downarrow}^{nX}(k) + T_{+\downarrow}^{pX}(k) T_{+\uparrow}^{nX}(k) \right] \right. \\
& \left. + v^2 \frac{3}{5} |Y_{21}|^2 \left[T_{+\uparrow}^{pX}(k) T_{+\uparrow}^{nX}(k) + T_{+\downarrow}^{pX}(k) T_{+\downarrow}^{nX}(k) \right] \right\}. \quad (84c)
\end{aligned}$$

On the other hand the form factors for the polarized deuteron

$$S_H(\mathbf{k}) = \int d^3 r |\psi_H(\mathbf{r})|^2 e^{i\mathbf{k} \cdot \mathbf{r}} \quad (85)$$

read:

$$\begin{aligned}
S_+(\mathbf{k}) = S_-(\mathbf{k}) = & \int d^3 r e^{i\mathbf{k} \cdot \mathbf{r}} \frac{1}{\mathbf{r}^2} \\
& \times \left\{ u^2 |Y_{00}|^2 + uv \frac{1}{\sqrt{10}} (Y_{00}^* Y_{20} + c.c.) + v^2 \left[\frac{1}{10} |Y_{20}|^2 + \frac{3}{5} |Y_{22}|^2 + \frac{3}{10} |Y_{21}|^2 \right] \right\}, \quad (86a)
\end{aligned}$$

$$\begin{aligned}
S_0(\mathbf{k}) = & \int d^3 r e^{i\mathbf{k} \cdot \mathbf{r}} \frac{1}{\mathbf{r}^2} \\
& \times \left\{ u^2 |Y_{00}|^2 - uv \frac{2}{\sqrt{10}} (Y_{00}^* Y_{20} + c.c.) + v^2 \frac{2}{5} |Y_{20}|^2 + \frac{3}{5} v^2 |Y_{21}|^2 \right\}. \quad (86b)
\end{aligned}$$

REFERENCES

- [1] SMC Collab., D. Adams et al., Phys. Lett. **B396** (1997) 338; Phys. Lett. **B357** (1995) 248
- [2] E142 Collab., P.L. Anthony et al., Phys. Rev. **D54** (1996) 6620
- [3] E143 Collab., K. Abe et al., Phys. Lett. **B364** (1995) 61; Phys. Rev. Lett. **75** (1995) 25
- [4] HERMES Collab., A. Simon et al., *Proc. Spin 96, Amsterdam, 1996*
- [5] M. Arneodo, Phys. Rep. **240** (1994) 301; D.F. Geesaman, S. Saito and A.W. Thomas, Ann. Rev. Nucl. Part. Sci. **45** (1995) 337
- [6] E665 Collab., M.R. Adams et al., Phys. Rev. Lett. **75** (1995) 1466
- [7] E665 Collab., M.R. Adams et al., Z. Phys. **C67** (1995) 403
- [8] NMC Collab., P. Amaudruz et al., Nucl. Phys. **B441** (1995) 3; A. Arneodo et al., Nucl. Phys. **B441** (1995) 12
- [9] P. Hoodbhoy, R.L. Jaffe and A. Manohar, Nucl. Phys. **B312** (1989) 571
- [10] G.A. Miller, *Proc. Electronuclear Physics with Internal Targets, Stanford, 1989*, edited by R.G. Arnold, World Scientific, Singapore, 1989
- [11] E. Sather and C. Schmidt, Phys. Rev. **D42** (1990) 1424
- [12] H.E. Jackson, *Proc. 11th Int. Symp. on High Energy Spin Physics, Bloomington, 1994*, AIP Conf. Proc. **339**
- [13] H. Khan and P. Hoodbhoy, Phys. Rev. **C44** (1991) 1219; A.Y. Umnikov, Phys. Lett. **B391** (1997) 177
- [14] H. Khan and P. Hoodbhoy, Phys. Lett. **B298** (1993) 181
- [15] J. Edelmann, G. Piller and W. Weise, Z. Phys. **A357** (1997) 129
- [16] N.N. Nikolaev and W. Schäfer, Phys. Lett. **B398** (1997) 254
- [17] J.F. Germond and C. Wilkin, Phys. Lett. **B59** (1975) 317
- [18] M. Strikman, *Proc. Symp. on Spin Structure of the Nucleon, Yale, 1994*, edited by V.H. Hughes and C. Cavata, World Scientific, Singapore, 1995
- [19] L. Frankfurt, V. Guzey and M. Strikman, Phys. Lett. **B381** (1996) 379
- [20] R.J. Glauber, *Lecture Notes in Theoretical Physics*, edited by W.E. Brittin et al., Interscience Publishers, New York, 1959
- [21] V.N. Gribov, JETP **29** (1969) 483, JETP **30** (1970) 709
- [22] L. Bertocchi, Nuovo Cim. **11A** (1972) 45; J.H. Weis, Acta Physica Polonica **B7** (1976) 851
- [23] S.A. Kulagin, W. Melnitchouk, G. Piller and W. Weise, Phys. Rev. **C52** (1995) 932; W. Melnitchouk and A.W. Thomas, Phys. Lett. **B377** (1996) 11; G. Piller, W. Melnitchouk and A. W. Thomas, Phys. Rev. **C54** (1996) 894
- [24] G. Piller, W. Ratzka and W. Weise, Z. Phys. **A352** (1995) 427
- [25] A. Donnachie and P.V. Landshoff, Phys. Lett. **B185** (1987) 403
- [26] L. Frankfurt and M. Strikman, Nucl. Phys. **B316** (1989) 340
- [27] T.H. Bauer, R.D. Spital, D.R. Yennie and F.M. Pipkin, Rev. Mod. Phys. **50** (1978) 261
- [28] T. J. Chapin et al., Phys. Rev. **D31** (1985) 17
- [29] ZEUS Collab., J. Breitweg et al., *Measurement of the diffractive structure function $F_2^{D(4)}$ at HERA*, hep-ex/9709021
- [30] J. Crittenden, Tracts in Modern Physics, Volume 140, Springer, 1997
- [31] M. Lacombe, B. Loiseau, J.M. Richard and R.V. Mau, Phys. Rev. **C21** (1980) 861
- [32] R. Machleidt, K. Holinde and C. Elster, Phys. Rep. **149** (1987) 1

- [33] NMC Collab., M. Arneodo et al., Nucl. Phys. **B 481** (1996) 3
- [34] B. Badelek and J. Kwiecinski, Nucl. Phys. **B 370** (1992) 278; W. Melnitchouk and A. W. Thomas, Phys. Lett. **B 317** (1993) 437; G. Piller, G. Niesler and W. Weise, Z. Phys. **A358** (1997) 407
- [35] K. Goulianos, Phys. Rep. **101** (1983) 169
- [36] L. Mankiewicz, Phys. Rev. **D40** (1989) 255; F. Close and S. Kumano, Phys. Rev. **D42** (1990) 2377
- [37] B. Badelek et al., J. Phys. **G22** (1996) 815-870
- [38] E665 Collab., M.R. Adams et al., Phys. Rev. **D54** (1996) 3006
- [39] NMC Collab., M. Arneodo et al., Nucl. Phys. **B483** (1997) 3
- [40] G. Baum et al., *COMPASS proposal*, CERN-SPSLC-96-14, 1996.

FIGURES

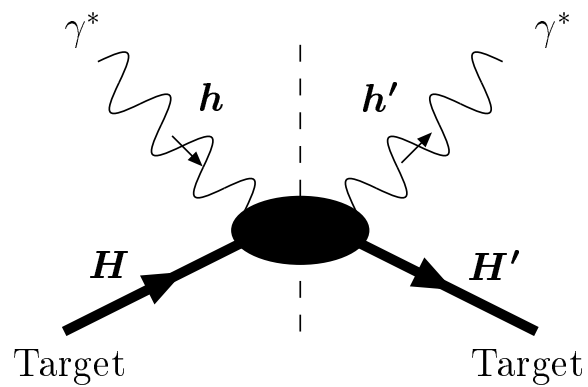


FIG. 1. Forward helicity amplitude for Compton scattering on a polarized target.

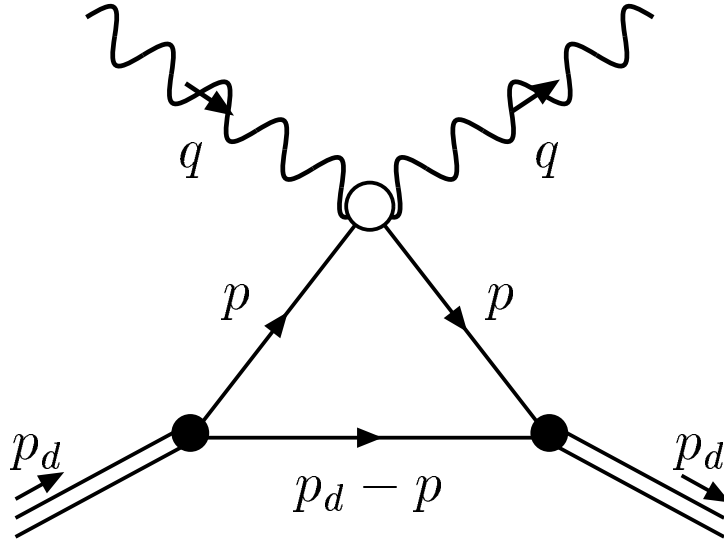


FIG. 2a. Single scattering contribution to virtual photon-deuteron scattering.

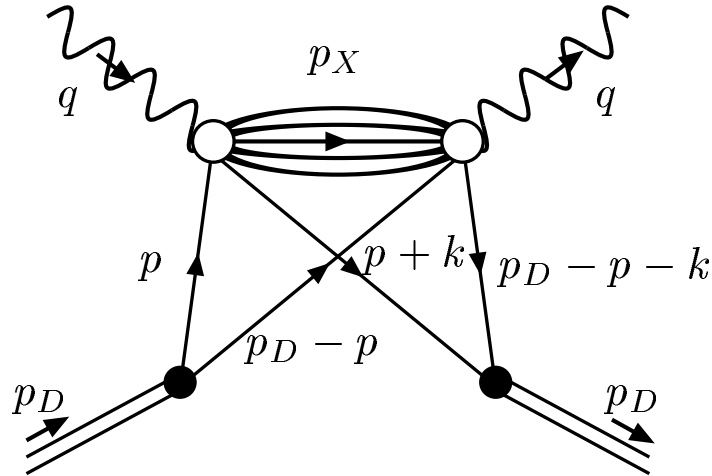


FIG. 2b. Double scattering contribution to virtual photon-deuteron scattering.

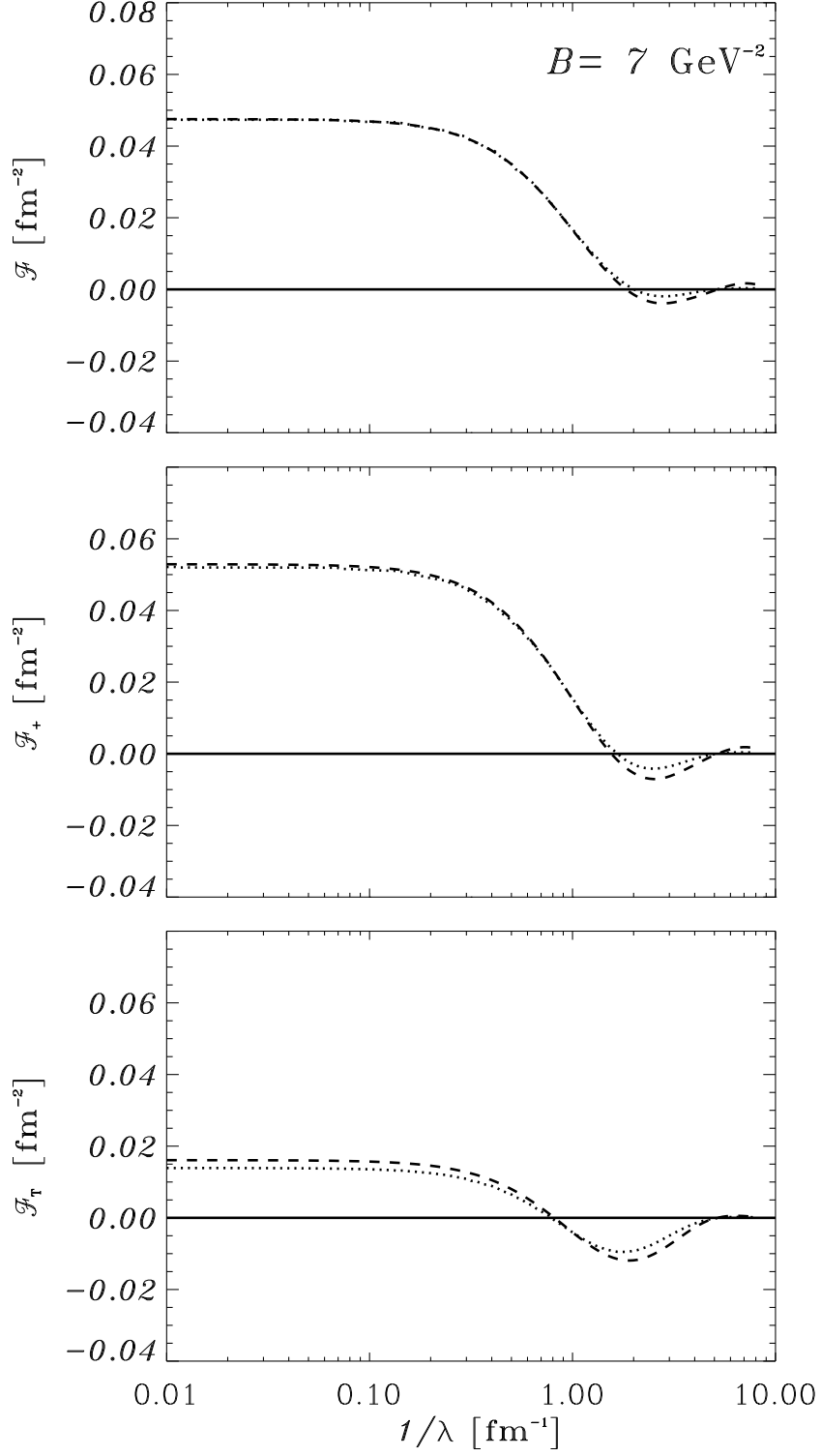


FIG. 3a. Integrated deuteron form factor \mathcal{F}_H from Eqs.(23,24,25) for different deuteron polarizations for an average slope $B = 7 \text{ GeV}^{-2}$. The dotted and dashed curves correspond to the Bonn [28] and Paris potential [27], respectively.

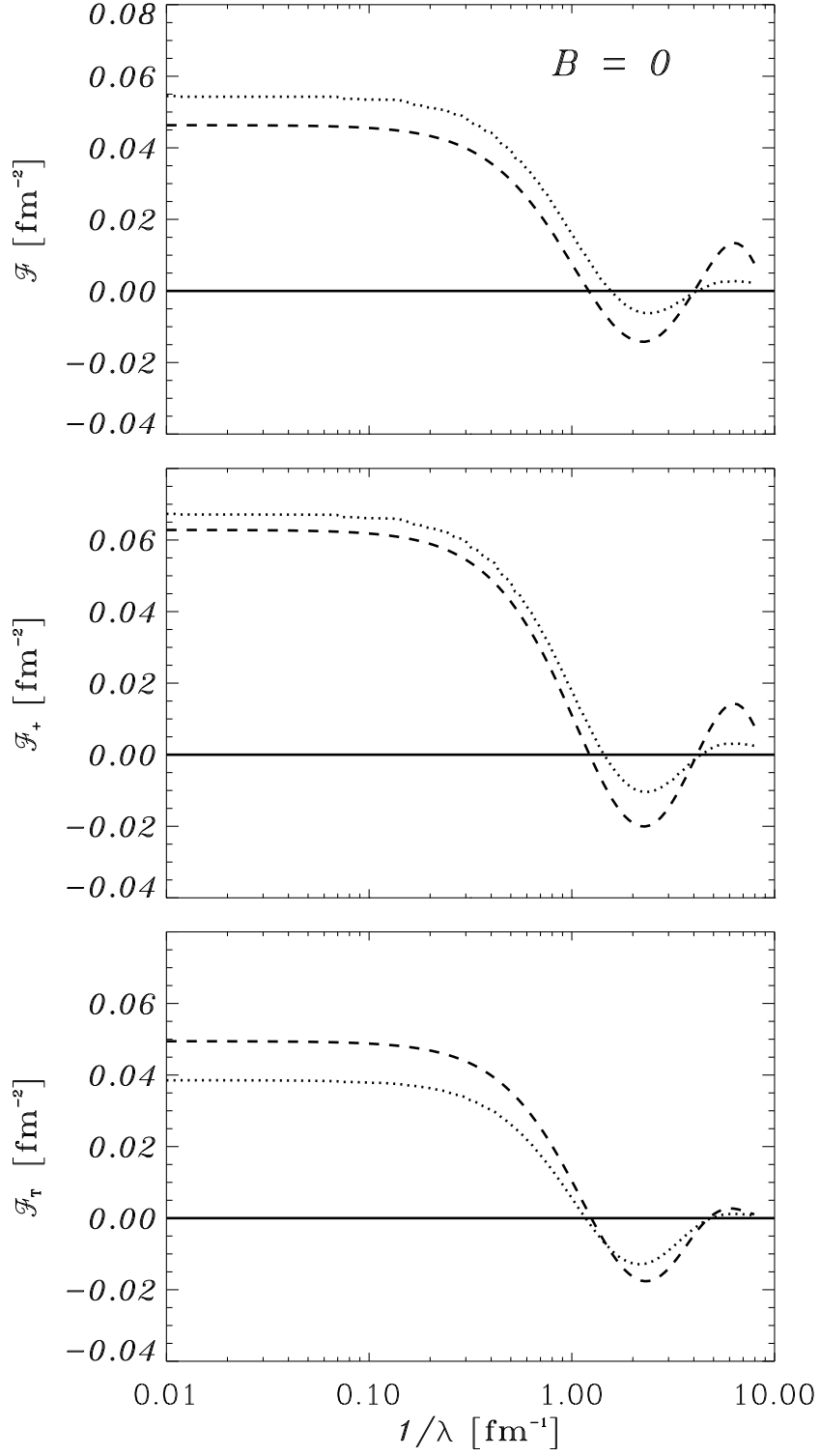


FIG. 3b. Integrated deuteron form factor \mathcal{F}_H from Eqs.(23,24,25) for different deuteron polarizations for an average slope $B = 0$. The dotted and dashed curves correspond to the Bonn [28] and Paris potential [27], respectively.

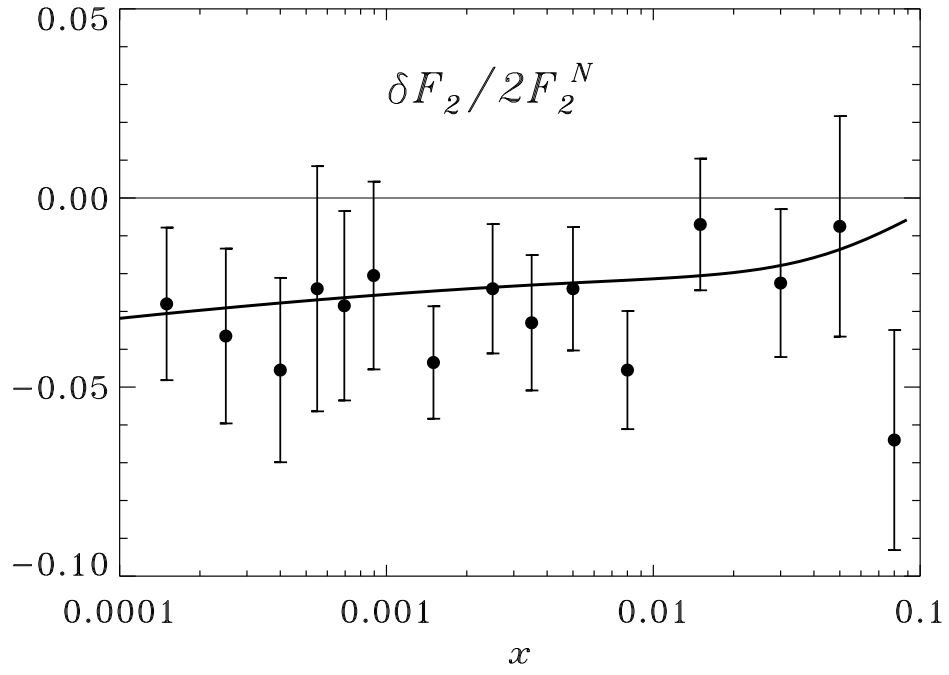


FIG. 4. Shadowing correction $\delta F_2/2F_2^N$ for deuterium, with data from E665 [6]. The full line represents a fit to the data used in (43) and (44).

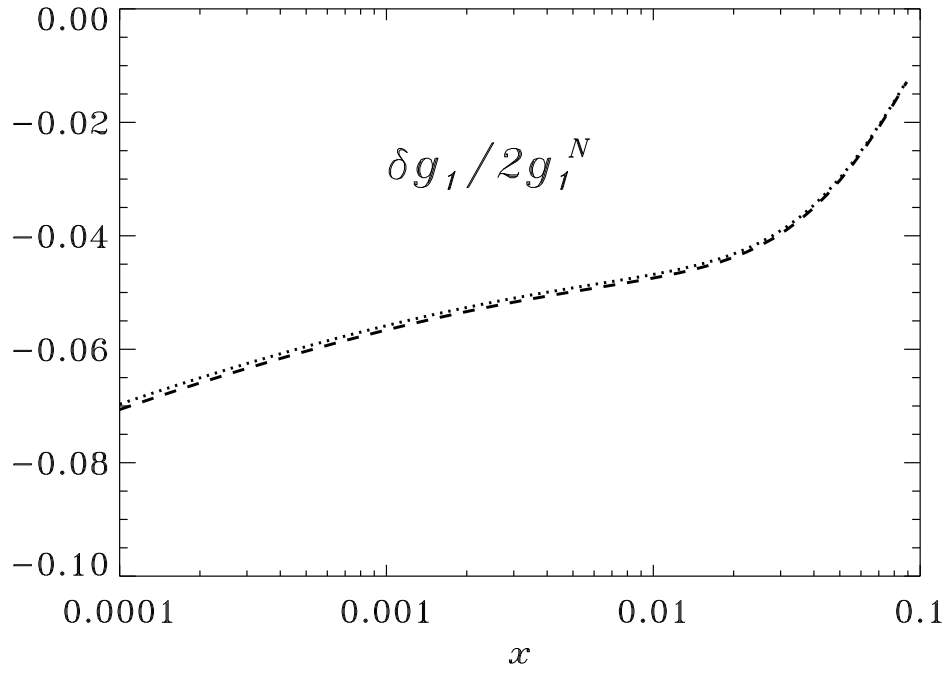


FIG. 5. Shadowing correction $\delta g_1/2g_1^N$ for deuterium. The dotted and dashed curves correspond to the Bonn OBE [28] and Paris potential [27], respectively.

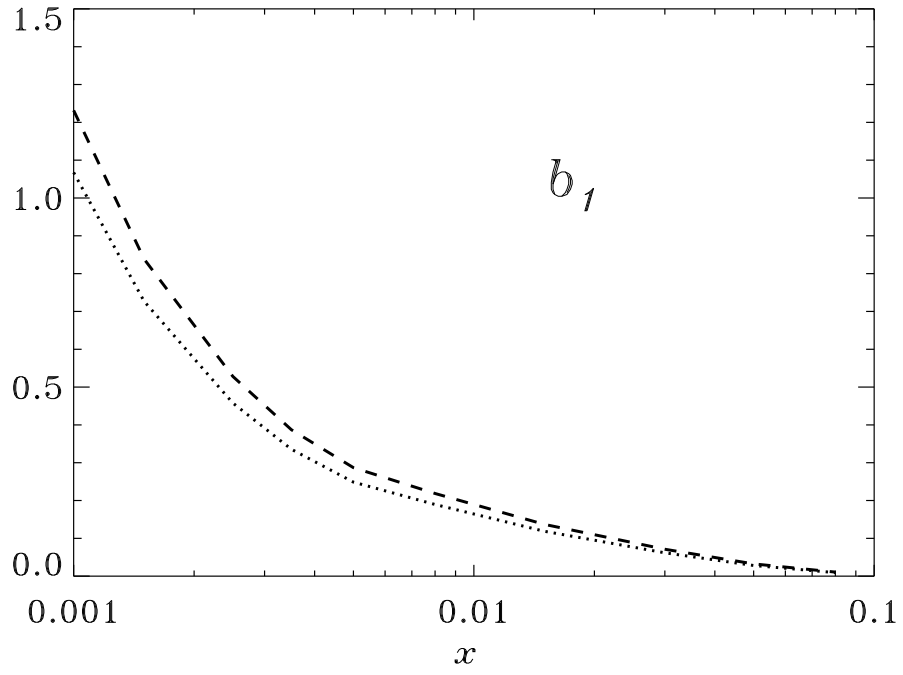


FIG. 6. Double scattering contribution to the tensor structure function b_1 of the deuteron. The dotted and dashed curves correspond to the Bonn OBE [28] and Paris potential [27], respectively.